



ISSN: 0067-2904

## The Peristaltic Flow of Jeffrey Fluid through a Flexible Channel

**Dheia G. Salih Al-Khafajy, Noor AL-Huda Kareem AL-Khalidi**

*Department of Mathematics, College of Science, University of Al-Qadisiyah, Diwaniya, Iraq*

Received: 17/2/2022

Accepted: 3/6/2022

Published: 30/12/2022

### Abstract

The purpose of this study is to calculate the effect of the elastic wall of a hollow channel of Jeffrey's fluid by peristaltic flow through two concentric cylinders. The inside tube is cylindrical and the outside is a regular elastic wall in the shape of a sine wave. Using the cylindrical coordinates and assuming a very short wavelength relative to the width of the channel to its length and using governing equations for Jeffrey's fluid in Navier-Stokes equations, the results of the problem are obtained. Through the Mathematica program these results are analysed.

**Keywords:** Jeffrey fluid, peristaltic flow, wall properties, cylindrical coordinates.

### التدفق التمعجي لمائع جيفري عبر قناة مرنة

**ضياء غازي صالح الخفاجي و نور الهدى كريم الخالدي**

قسم الرياضيات ، كلية العلوم ، جامعة القادسية ، الديوانية ، العراق

### الخلاصة

الغرض من هذه الدراسة هو حساب تأثير الجدار المرن لقناة مجوفة لسائل جيفري عن طريق التدفق التمعجي عبر أسطوانتين متحدتين المركز، الأنبوب الداخلي أسطواني والخارج جدار مرن منتظم على شكل موجة جيبيية. باستخدام الإحداثيات الأسطوانية وافترض طول موجي قصير جداً "بالنسبة لعرض القناة لطولها" وباستخدام المعادلات الحاكمة لسائل جيفري في معادلات نافير-ستوكس، تم الحصول على نتائج المشكلة ومن خلال برنامج "Mathematica" تم تحليل النتائج.

## 1. Introduction

Peristalsis is a way of transporting fluid through the contraction process on the wall of the duct. This process has several very important uses in most industry and biological systems, for example, the movement of food through the esophagus, movement of chyme in the digestive tract, movement of veins, capillaries, arteries in blood vessels, the process of transporting urine from the kidneys to the bladder and others. Because of the importance of peristaltic flows in living organisms (the structure of humans and animals) in addition to their entry into the manufacture of various types of biological products and others, research has been taken to develop in this direction and the most of it was in Cartesian coordinates. One of the first researchers is Latham [1], his work was on liquid motions in a peristaltic pump. Shapiro et al. [2] presented a paper entitled peristaltic pumping at long wavelengths at low

\*Email: [dr.dheia.g.salih@gmail.com](mailto:dr.dheia.g.salih@gmail.com)

Reynolds number, and Chin-Hsiu [3] discussed peristaltic transport in circular cylindrical tubes.

Then, Nadeem et al. [4] presented a paper entitled peristaltic flow of Jeffrey's liquid in a rectangular duct having compliant walls. Al-Khafajy [5] studied magnetohydrodynamic peristaltic flow of couple stress with heat and mass transfer of a Jeffrey fluid in a tube through a porous medium. Al-Aridhee and Al-Khafajy [6] discussed the influence of MHD peristaltic transport for Jeffrey fluid with varying temperature and concentrations through a porous medium. Salman and Ali [7] presented their study on the combined effects and heat transfer of the porous medium of the Jeffrey cradle fluid flowing through a two-dimensional asymmetric, pointed oblique channel, in their work, the results show a parabolic behavior, it rises in the central part of the channel and decreases due to the effect of Hartmann's number, while the opposite behavior is through the effect of the porosity modulus. Almusawi and Abdulhadi [8] presented and discussed Ree–Eyring fluid's peristaltic transport in a rotating frame and examined the impacts of magnetohydrodynamics.

Al-khafajy and Abd Alhadi [9] studied the effects of wall properties and heat transfer on the peristaltic transport of Jeffrey fluid through a porous medium channel. Sankad and Nagathan [10] studied the influence of wall properties on the peristaltic flow of Jeffrey fluid in a uniform porous channel under heat transfer. Eldesoky et al. [11] studied the combined influences of heat transfer and compliant properties of wall and slip conditions on the peristaltic flow through tube. Recently, Al-Waily and Al-khafajy [12] presented a paper entitled magnetohydrodynamics peristaltic flow of a couple-stress for a Jeffrey fluid through a flexible porous medium.

We present this study with the motivation of searching the study of the effect of a peristaltic flow of Jeffrey fluid through a channel of two overlapping tubes, the inside tube is cylindrical and the outside a regular elastic channel in the shape of a sine wave by cylindrical coordinates.

## 2. Mathematical Formulation

Consider the peristaltic flow of Jeffrey fluid through two concentric cylinders, the inside tube is cylindrical and the outside is a regular elastic wall in the shape of a sine wave. The cylindrical coordinates are represented by  $R$  along the radius of the tube and  $Z$  synchronously with the axis of the tube as in Figure 1. We know the geometry of the wall surface as follows;

Inner wall

$$\bar{r} = \bar{r}_1 = a_1$$

Outer wall

$$\bar{r} = \bar{r}_2(\bar{z}, \bar{t}) = a_2 + b \sin\left(\frac{2\pi}{\gamma}(\bar{z} - c\bar{t})\right)$$

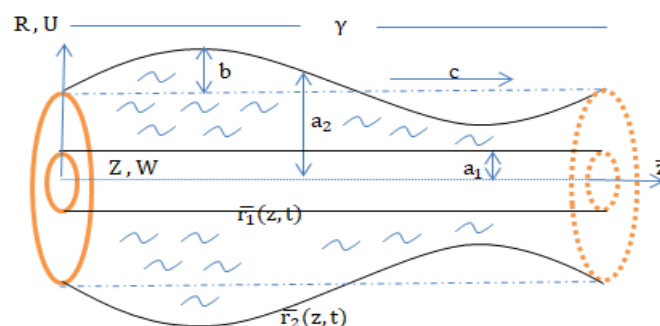


**Figure 1:** The problem Geometry

where  $a_2$  is the average radius of the undisturbed tube,  $b$  is the amplitude of a peristaltic wave,  $\gamma$  is a wavelength,  $c$  is a wave propagation speed, and  $\bar{t}$  represents the time.

**3. Constitutive Equations**

Basic equations governing continuity and the Navier-Stokes equations are

$$\nabla \bar{U} = 0, \tag{1}$$

$$\rho (\bar{U} \cdot \nabla) \bar{U} = \nabla \bar{J}, \tag{2}$$

respectively. Where  $\bar{U}$  = the velocity field,  $\rho$  = a density and  $\nabla \bar{U}$  = the fluid velocity gradient. The constituent equations of Jeffery's non-compressible fluid are given by:

$$\bar{J} = -\bar{p}\bar{I} + \bar{S} \tag{3}$$

$$\bar{S} = \frac{\mu}{1+\lambda_1} \left( \bar{\beta} + \lambda_2 \bar{\dot{\beta}} \right) \tag{4}$$

where  $\bar{S}$  is the additional stress tensor,  $\bar{p}$  is pressure,  $\bar{I}$  is the identity Tensor,  $\lambda_1$  is the ratio of relaxation to lag times,  $\bar{\beta}$  is the shear ratio,  $\bar{\dot{\beta}}$  is derived materials and  $\lambda_2$  is retardation time.

Let  $\bar{U} = (u_1, u_2, u_3)$  be the velocity vector at cylindrical coordinates  $(r, \vartheta, z)$ . The shear strain tensor is illustrated as follows:

$$\dot{\beta} = 2E = \begin{bmatrix} 2 \frac{\partial u_1}{\partial r} & \frac{1}{r} \left( \frac{\partial u_1}{\partial \vartheta} - u_2 + r \frac{\partial u_2}{\partial r} \right) & \frac{\partial u_1}{\partial z} + \frac{\partial u_3}{\partial r} \\ \frac{1}{r} \left( \frac{\partial u_1}{\partial \vartheta} - u_2 + r \frac{\partial u_2}{\partial r} \right) & \frac{2}{r} \left( \frac{\partial u_2}{\partial \vartheta} + u_1 \right) & \frac{\partial u_2}{\partial z} + \frac{1}{r} \frac{\partial u_3}{\partial \vartheta} \\ \frac{\partial u_1}{\partial z} + \frac{\partial u_3}{\partial r} & \frac{\partial u_2}{\partial z} + \frac{1}{r} \frac{\partial u_3}{\partial \vartheta} & 2 \frac{\partial u_3}{\partial z} \end{bmatrix}$$

and  $\dot{\beta} = \frac{D\dot{\beta}}{Dt} = \frac{\partial \dot{\beta}}{\partial t} + \nabla \nabla \dot{\beta}$  "material derivative".

**4. Flexible wall**

We can express the governing equation of the elastic wall by the following formula [9]  $L^{**} = \bar{P} - \bar{p}_0$ . So that it is used to represent the motion of the stretched membrane with the viscosity of the damping force so that

$$L^{**} = B \frac{\partial^4}{\partial \bar{z}^4} - C \frac{\partial^2}{\partial \bar{z}^2} + m \frac{\partial^2}{\partial \bar{t}^2} + D \frac{\partial}{\partial \bar{t}} + A_L.$$

where  $B, C, m, D,$  and  $A_L$  are the flexural rigidity of the wall, the longitudinal tension per unit width, the mass per unit area, the coefficient of viscous damping, and the spring stiffness, respectively.

The governing equation that is used for duct characteristics for the wall in  $\bar{r} = \bar{k}$ , it is found;  $\frac{\partial \bar{P}}{\partial \bar{z}} = \frac{\partial}{\partial \bar{z}} \left( B \frac{\partial^4}{\partial \bar{z}^4} - C \frac{\partial^2}{\partial \bar{z}^2} + m \frac{\partial^2}{\partial \bar{t}^2} + D \frac{\partial}{\partial \bar{t}} + A_L \right) (\bar{k})$ .

**5. Method of solution**

We write the speed components in an unstable two-dimensional flow as follows:  $\bar{U} = (\bar{U}_1(\bar{r}, \bar{z}, \bar{t}), 0, \bar{U}_3(\bar{r}, \bar{z}, \bar{t}))$ , here  $\bar{U}_1$  and  $\bar{U}_3$  represent speed components corresponding to the radial and axial direction in a given frame, respectively.

The governing equations are got for fluid motion after replacing the velocity components in the shear stress equations for Jeffrey fluid, then in Eq. (1) and Eq.(2), we have

$$\frac{\partial \bar{U}_1}{\partial \bar{R}} + \frac{\bar{U}_1}{\bar{R}} + \frac{\partial \bar{U}_3}{\partial \bar{Z}} = 0 \tag{5}$$

$$\rho \left( \frac{\partial \bar{U}_1}{\partial \bar{t}} + \bar{U}_1 \frac{\partial \bar{U}_1}{\partial \bar{R}} + \bar{U}_3 \frac{\partial \bar{U}_1}{\partial \bar{Z}} \right) = -\frac{\partial \bar{p}}{\partial \bar{R}} + \frac{1}{\bar{R}} \frac{\partial}{\partial \bar{R}} (\bar{R} \bar{S}_{RR}) + \frac{\partial}{\partial \bar{Z}} (\bar{S}_{RZ}) \tag{6}$$

$$\rho \left( \frac{\partial \bar{U}_3}{\partial \bar{t}} + \bar{U}_1 \frac{\partial \bar{U}_3}{\partial \bar{R}} + \bar{U}_3 \frac{\partial \bar{U}_3}{\partial \bar{Z}} \right) = - \frac{\partial \bar{p}}{\partial \bar{Z}} + \frac{1}{\bar{R}} \frac{\partial}{\partial \bar{R}} (\bar{R} \bar{S}_{\bar{R}\bar{Z}}) + \frac{\partial}{\partial \bar{Z}} (\bar{S}_{\bar{Z}\bar{Z}}) \tag{7}$$

and the components of the extra stress are;

$$\bar{S}_{\bar{R}\bar{R}} = \frac{2\mu}{1+\lambda_1} \left( \frac{\partial \bar{U}_1}{\partial \bar{R}} + \lambda_2 \left( \frac{\partial^2 \bar{U}_1}{\partial \bar{R} \partial \bar{t}} + \bar{U}_1 \frac{\partial^2 \bar{U}_1}{\partial \bar{R}^2} + \bar{U}_3 \frac{\partial^2 \bar{U}_1}{\partial \bar{R} \partial \bar{Z}} \right) \right) \tag{8}$$

$$\bar{S}_{\bar{R}\bar{Z}} = \frac{\mu}{1+\lambda_1} \left( \frac{\partial \bar{U}_1}{\partial \bar{Z}} + \frac{\partial \bar{U}_3}{\partial \bar{R}} + \lambda_2 \left( \frac{\partial^2 \bar{U}_1}{\partial \bar{Z} \partial \bar{t}} + \frac{\partial^2 \bar{U}_3}{\partial \bar{R} \partial \bar{t}} \right) + \lambda_2 \left( \bar{U}_1 \left( \frac{\partial^2 \bar{U}_1}{\partial \bar{R} \partial \bar{Z}} + \frac{\partial^2 \bar{U}_3}{\partial \bar{R}^2} \right) + \bar{U}_3 \left( \frac{\partial^2 \bar{U}_1}{\partial \bar{Z}^2} + \frac{\partial^2 \bar{U}_3}{\partial \bar{R} \partial \bar{Z}} \right) \right) \right) \tag{9}$$

$$\bar{S}_{\bar{\theta}\bar{\theta}} = \frac{2\mu}{1+\lambda_1} \frac{1}{\bar{R}} \left( \bar{U}_1 + \lambda_2 \left( \frac{\partial \bar{U}_1}{\partial \bar{t}} - \frac{\bar{U}_1}{\bar{R}} \left( \bar{U}_1 - \bar{R} \frac{\partial \bar{U}_1}{\partial \bar{R}} \right) + \bar{U}_3 \frac{\partial \bar{U}_1}{\partial \bar{Z}} \right) \right) \tag{10}$$

$$\bar{S}_{\bar{Z}\bar{Z}} = \frac{2\mu}{1+\lambda_1} \left( \frac{\partial \bar{U}_3}{\partial \bar{Z}} + \lambda_2 \left( \frac{\partial^2 \bar{U}_3}{\partial \bar{Z} \partial \bar{t}} + \bar{U}_1 \frac{\partial^2 \bar{U}_3}{\partial \bar{R} \partial \bar{Z}} + \bar{U}_3 \frac{\partial^2 \bar{U}_3}{\partial \bar{Z}^2} \right) \right) \tag{11}$$

The corresponding boundary conditions are:

$$\left. \begin{aligned} \bar{U}_3 = 0, \bar{U}_1 = 0 \quad \text{at } \bar{r} = \bar{r}_1 = a_1 \\ \bar{U}_3 = 0, \bar{U}_1 = 0 \quad \text{at } \bar{r} = \bar{r}_2(\bar{z}, \bar{t}) = a_2 + b \sin\left(\frac{2\pi}{\gamma}(\bar{z} - c\bar{t})\right) \end{aligned} \right\} \tag{12}$$

General and special two-frame coordinate transformations are given as follows:  $\bar{r} = \bar{R}$ ,  $\bar{z} = \bar{Z}$ ,  $\bar{u}_1 = \bar{U}_1$ , and  $\bar{u}_3 = \bar{U}_3 - c$

For  $(\bar{u}_1, \bar{u}_3)$  and  $(\bar{U}_1, \bar{U}_3)$  represent the speed components in fixed and the moving tires, respectively. After using these transitions, we have

$$\frac{\partial \bar{u}_1}{\partial \bar{r}} + \frac{\bar{u}_1}{\bar{r}} + \frac{\partial(\bar{u}_3+c)}{\partial \bar{z}} = 0 \tag{13}$$

$$\rho \left( \frac{\partial \bar{u}_1}{\partial \bar{t}} + \bar{u}_1 \frac{\partial \bar{u}_1}{\partial \bar{r}} + (\bar{u}_3 + c) \frac{\partial \bar{u}_1}{\partial \bar{z}} \right) = - \frac{\partial \bar{p}}{\partial \bar{r}} + \frac{1}{\bar{r}} \frac{\partial}{\partial \bar{r}} (\bar{r} \bar{S}_{\bar{r}\bar{r}}) + \frac{\partial}{\partial \bar{z}} (\bar{S}_{\bar{r}\bar{z}}) \tag{14}$$

$$\rho \left( \frac{\partial(\bar{u}_3+c)}{\partial \bar{t}} + \bar{u}_1 \frac{\partial(\bar{u}_3+c)}{\partial \bar{r}} + (\bar{u}_3 + s) \frac{\partial(\bar{u}_3+c)}{\partial \bar{z}} \right) = - \frac{\partial \bar{p}}{\partial \bar{z}} + \frac{1}{\bar{r}} \frac{\partial}{\partial \bar{r}} (\bar{r} \bar{S}_{\bar{r}\bar{z}}) + \frac{\partial}{\partial \bar{z}} (\bar{S}_{\bar{z}\bar{z}}) \tag{15}$$

with the governing motion equation on the elastic wall, we get

$$\frac{\partial}{\partial \bar{z}} \left( B \frac{\partial^4}{\partial \bar{z}^4} - C \frac{\partial^2}{\partial \bar{z}^2} + m \frac{\partial^2}{\partial \bar{t}^2} + D \frac{\partial}{\partial \bar{t}} + A_L \right) (\bar{k}) = \frac{\partial \bar{p}}{\partial \bar{z}} = -\rho \left( \frac{\partial(\bar{u}_3+c)}{\partial \bar{t}} + \bar{u}_1 \frac{\partial(\bar{u}_3+c)}{\partial \bar{r}} + (\bar{u}_3 + c) \frac{\partial(\bar{u}_3+c)}{\partial \bar{z}} \right) + \frac{1}{\bar{r}} \frac{\partial}{\partial \bar{r}} (\bar{r} \bar{S}_{\bar{r}\bar{z}}) + \frac{\partial}{\partial \bar{z}} (\bar{S}_{\bar{z}\bar{z}}) \tag{16}$$

We present the following dimensionless transformations for the purpose of simplifying the governing equations of motion

$$\left. \begin{aligned} u_1 = \frac{\bar{u}_1 \gamma}{a_2 c}, \quad u_3 = \frac{\bar{u}_3}{c}, \quad r = \frac{\bar{r}}{a_2}, \quad z = \frac{\bar{z}}{\gamma}, \quad S = \frac{a_2 \bar{S}}{\mu c}, \quad \delta = \frac{a_2}{\gamma}, \quad p = \frac{a_2^2 \bar{p}}{\mu c \gamma}, \quad t = \frac{c \bar{t}}{\gamma}, \\ r_1 = \frac{\bar{r}_1}{a_2} = \varepsilon < 1, \quad \phi = \frac{b}{a_2}, \quad r_2 = \frac{\bar{r}_2}{a_2} = 1 + \phi \sin(2\pi \bar{z}), \quad Re = \frac{\rho c a_2}{\mu} \end{aligned} \right\} \tag{17}$$

where  $\phi$  = "amplitude ratio",  $Re$  = "Reynolds number" and  $\delta$  = "dimensionless wave number".

Substituting equation (17) into the components of the extra stress equations (8-11), equations (13-16), and the boundary conditions (12), respectively. We have

$$\left(\frac{c}{\gamma}\right) \left( \frac{\partial u_1}{\partial r} + \frac{u_1}{r} + \frac{\partial u_3}{\partial z} \right) = 0 \tag{18}$$

$$Re \delta^3 \left( \frac{\partial u_1}{\partial t} + u_1 \frac{\partial u_1}{\partial r} + (u_3 + 1) \frac{\partial u_1}{\partial z} \right) = - \frac{\partial p}{\partial r} + \delta \frac{1}{r} \frac{\partial}{\partial r} (r S_{rr}) + \delta^2 \frac{\partial}{\partial z} (S_{rz}) \tag{19}$$

$$Re \delta \left( \frac{\partial u_3}{\partial t} + u_1 \frac{\partial u_3}{\partial r} + (u_3 + 1) \frac{\partial u_3}{\partial z} \right) = - \frac{\partial p}{\partial z} + \frac{1}{r} S_{rz} + \frac{\partial}{\partial r} (S_{rz}) + \delta \frac{\partial}{\partial z} (S_{zz}) \tag{20}$$

And the equation of motion governing the elastic wall

$$\left(\frac{Ba_2^3}{\mu c \gamma^5}\right) \frac{\partial^5(k)}{\partial z^5} - \left(\frac{Ca_2^3}{\mu c \gamma^3}\right) \frac{\partial^3(k)}{\partial z^3} + \left(\frac{mca_2^3}{\mu \gamma^3}\right) \frac{\partial^3(k)}{\partial z \partial t^2} + \left(\frac{Da_2^3}{\mu \gamma^2}\right) \frac{\partial^2(k)}{\partial z \partial t} + \left(\frac{A_L a_2^3}{\mu c \gamma}\right) \frac{\partial(k)}{\partial z} = -\text{Re } \delta \left(\frac{\partial u_3}{\partial t} + u_1 \frac{\partial u_3}{\partial r} + (u_3 + 1) \frac{\partial u_3}{\partial z}\right) + \frac{1}{r} S_{rz} + \frac{\partial}{\partial r} (S_{rz}) + \delta \frac{\partial}{\partial z} (S_{zz}) \tag{21}$$

where:

$$\begin{aligned} S_{rr} &= \frac{2\delta}{1+\lambda_1} \left[1 + \frac{c \lambda_2 \delta}{a_2} \left(\frac{\partial}{\partial t} + u_1 \frac{\partial}{\partial r} + (u_3 + 1) \frac{\partial}{\partial z}\right)\right] \left(\frac{\partial u_1}{\partial r}\right) \\ S_{rz} &= \frac{1}{1+\lambda_1} \left[1 + \frac{c \lambda_2 \delta}{a_2} \left(\frac{\partial}{\partial t} + u_1 \frac{\partial}{\partial r} + (u_3 + 1) \frac{\partial}{\partial z}\right)\right] \left(\frac{\partial u_3}{\partial r} + \delta^2 \frac{\partial u_1}{\partial z}\right) \\ S_{\theta\theta} &= \frac{2\delta}{1+\lambda_1} \left[\frac{u_1}{r} + \frac{c \lambda_2 \delta}{a_2} \left(\frac{1}{r} \frac{\partial u_1}{\partial t} + \frac{u_1}{r} \frac{\partial u_1}{\partial r} - \frac{u_1^2}{r^2} + (u_3 + 1) \frac{1}{r} \frac{\partial u_1}{\partial z}\right)\right] \\ S_{zz} &= \frac{2\delta}{1+\lambda_1} \left[1 + \frac{c \lambda_2 \delta}{a_2} \left(\frac{\partial}{\partial t} + u_1 \frac{\partial}{\partial r} + (u_3 + 1) \frac{\partial}{\partial z}\right)\right] \left(\frac{\partial u_3}{\partial z}\right) \end{aligned}$$

This gives boundary conditions with respect to dimensionless variables in the wave framework:

$$\left. \begin{aligned} u_3 = -1, u_1 = 0 & \quad \text{at } r = r_1 = \varepsilon \\ u_3 = -1, u_1 = 0 & \quad \text{at } r = r_2 = 1 + \phi \cdot \text{Sin}(2\pi(z-t)) \end{aligned} \right\} \tag{22}$$

**6. Solutions of the Problem**

The general solution of the equations (18-21) seems impossible, so we will limit the analysis to the assumption of a small number of dimensionless waves. So, it will follow  $\delta \ll 1$ . Another expression, by approximation we define the wavelengths. By our assumption, we get

$$\frac{\partial u_1}{\partial r} + \frac{u_1}{r} + \frac{\partial u_3}{\partial z} = 0 \tag{23}$$

$$\frac{\partial p}{\partial r} = 0 \tag{24}$$

$$\frac{\partial p}{\partial z} = \frac{1}{r} (S_{rz}) + \frac{\partial}{\partial r} (S_{rz}) \tag{25}$$

$$F_1 \frac{\partial^5(k)}{\partial z^5} - F_2 \frac{\partial^3(k)}{\partial z^3} + F_3 \frac{\partial^3(k)}{\partial z \partial t^2} + F_4 \frac{\partial^2(k)}{\partial z \partial t} + F_5 \frac{\partial(k)}{\partial z} = \frac{1}{r} S_{rz} + \frac{\partial}{\partial r} (S_{rz}) \tag{26}$$

where  $F_1 = \frac{Ba_2^3}{\mu c \gamma^5}$  is the flexural stiffness of the wall,  $F_2 = \frac{Ca_2^3}{\mu c \gamma^3}$  stands for the longitudinal tension per unit width,  $F_3 = \frac{mca_2^3}{\mu \gamma^3}$  represents the mass per unit area,  $F_4 = \frac{Da_2^3}{\mu \gamma^2}$  is the coefficient of viscid damping, and  $F_5 = \frac{A_L a_2^3}{\mu c \gamma}$  is the spring stiffness. The components of the extra stress, are  $S_{rr} = S_{\theta\theta} = S_{zz} = 0$  and  $S_{rz} = \frac{1}{1+\lambda_1} \left(\frac{\partial u_3}{\partial r}\right)$

Replacing the components of extra stress into equation (26), we have

$$\frac{1}{1+\lambda_1} \frac{1}{r} \frac{\partial}{\partial r} \left(r \frac{\partial u_3}{\partial r}\right) = \left(F_1 \frac{\partial^5(k)}{\partial z^5} - F_2 \frac{\partial^3(k)}{\partial z^3} + F_3 \frac{\partial^3(k)}{\partial z \partial t^2} + F_4 \frac{\partial^2(k)}{\partial z \partial t} + F_5 \frac{\partial(k)}{\partial z}\right) \tag{27}$$

A corresponding stream function  $u_1 = -\frac{1}{r} \frac{\partial \psi}{\partial z}$  and  $u_3 = \frac{1}{r} \frac{\partial \psi}{\partial r}$ .

**6.1 Momentum Equation**

Equation (27) can be written as follows:

$$\frac{1}{r} \frac{\partial}{\partial r} \left(r \frac{\partial u_3}{\partial r}\right) = B(1 + \lambda_1) \tag{28}$$

where  $B = \left(F_1 \frac{\partial^5(k)}{\partial z^5} - F_2 \frac{\partial^3(k)}{\partial z^3} + F_3 \frac{\partial^3(k)}{\partial z \partial t^2} + F_4 \frac{\partial^2(k)}{\partial z \partial t} + F_5 \frac{\partial(k)}{\partial z}\right)$

The closed form solution for the equation (28) with the boundary conditions equation (22) is given by:

$$u_3 = \frac{Br^2}{4} - \left(\frac{4\text{Log}[k]+B\epsilon^2\text{Log}[k]-4\text{Log}[\epsilon]-Bk^2\text{Log}[\epsilon]}{4(\text{Log}[k]-\text{Log}[\epsilon])}\right) - \left(\frac{Bk^2-B\epsilon^2}{4(\text{Log}[k]-\text{Log}[\epsilon])}\right) \text{Log}[r]$$

### 6.2 Shear Stress

The equation stress on a face  $r$  and acting in the direction  $z$  is

$$S_{rz} = \frac{1}{1+\lambda_1} \left( \frac{Br}{2} - \frac{Bk^2 - B\epsilon^2}{4r(\text{Log}[k] - \text{Log}[\epsilon])} \right)$$

### 6.3 Stream Function

The corresponding stream function is  $\psi = \int r u_3 dr$ , which is

$$\psi = r^2 \left( \frac{Bk^2 - B\epsilon^2 + (-8 + B(r^2 - 2\epsilon^2))\text{Log}[k]}{16(\text{Log}[k] - \text{Log}[\epsilon])} + \frac{2B(-k^2 + \epsilon^2)\text{Log}[r] + 8\text{Log}[\epsilon]}{16(\text{Log}[k] - \text{Log}[\epsilon])} + \frac{2Bk^2\text{Log}[\epsilon] - Br^2\text{Log}[\epsilon]}{16(\text{Log}[k] - \text{Log}[\epsilon])} \right)$$

## 7. Conclusions

The program Mathematica 12 has been used to discuss illustrations to study the effect of the peristaltic flow of Jeffrey fluid through a channel of two nested tubes, the inner tube is cylindrical, and the outer tube is regular elastic sine wave shape. Our study has been adopted cylindrical coordinates to simulate virtual reality. Figures 2-20 illustrate the parameters of results, the parameter  $F_1$  represents the flexural rigidity of the wall, the parameter  $F_2$  is longitudinal tension per unit width, the parameter  $F_3$  stands for the mass per unit area, the parameter  $F_4$  is the coefficient of viscous damping, the parameter  $F_5$  is the spring stiffness, the parameter  $\lambda_1$  is the ratio of relaxation to retardation times, the parameter  $\phi$  is the amplitude ratio and the parameter  $\epsilon$  represents the inner cylinder (tube) radius on the peristaltic flow for Jeffrey's fluid through the channel that we have indicated.

### 7.1 Velocity Distribution

Figures 2-3 illustrate the parameters of the results  $F_1, F_2, F_3, F_4, F_5, \epsilon, \phi$  and  $\lambda_1$  on the distribution of velocity  $u_3$  vs.  $r$ , respectively. Figure 2a, displays the effect of  $F_1$  and  $F_2$  on a velocity distribution, we notice an increase in the velocity with increasing  $F_1$  and  $F_2$ , respectively. Figure 2b, shows that a velocity distribution increases with an increasing in parameters  $\lambda_1$  and  $\phi$ , respectively. In Figure 3a, we observed that the velocity distribution rises with an increasing in parameter  $F_5$  and decreases with increasing  $\epsilon$ . Figure 3b, shows the behavior of  $u_3$  under the effect of  $F_3$  and  $F_4$ , we notice that the velocity decreases when an increasing in  $F_3$  and  $F_4$ , respectively.

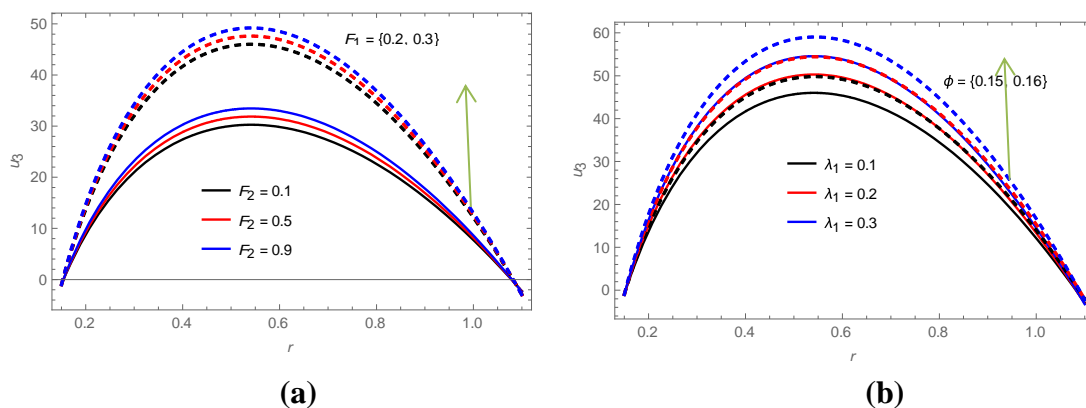


**Figure 2:** Velocity distribution for various values of (a)  $F_1$  and  $F_2$ , (b)  $\lambda_1$  and  $\phi$  for constant values of parameter  $\epsilon = 0.15, F_3 = 0.1, z = 0.5, F_4 = 0.5, F_5 = 0.1, t = 0.1$

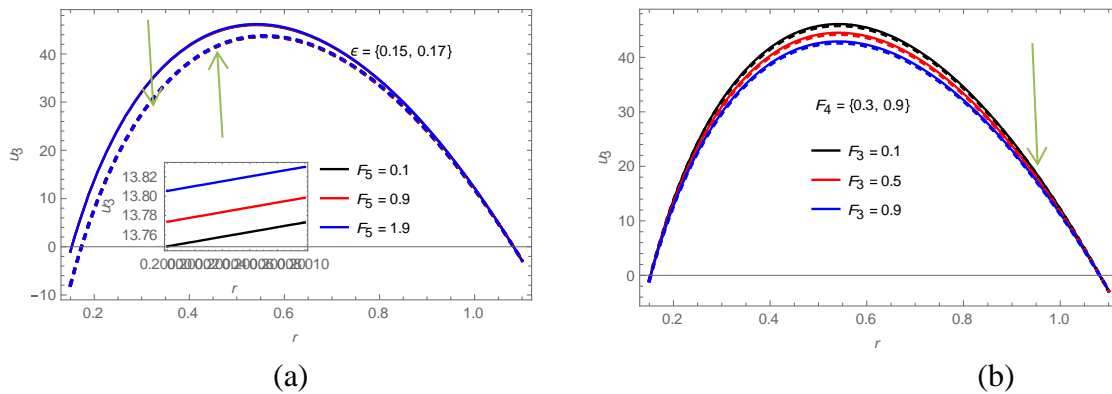


**Figure 3:** Velocity distribution for various values of(a)  $\epsilon$  and  $F_5$  ,(b)  $F_3$  and  $F_4$  for constant values of parameters  $F_1 = 0.3, \phi = 0.15, z = 0.5, F_2 = 0.1, \lambda_1 = 0.1, t = 0.1$

**7.2 Shear Stress**

Figures 4-5 illustrate the parameters of results  $F_1, F_2, F_5, F_3, F_4, \epsilon, \phi$ , and  $\lambda_1$  on the distribution of stress  $S_{rz}$ , respectively. Figure 4(a, b, c) displays an effect of the parameters  $F_1, F_2$ , and  $F_5$  on stress distribution, respectively. The stress is direct with these parameters in the region  $r < 0.55$ , while it has an inverse effect in the region  $r > 0.55$ , where in the first region the stress is positive. Otherwise, it is negative. In Figure 4d, we notice that the effect of the parameter  $\phi$  is similar to the effect of the parameter  $F_1$  on the stress distribution. Figure 5(a, b) shows the behavior of stress under the effect of the two parameters  $F_3$  and  $F_4$ , respectively. The stress is inversed with these two parameters in the region  $r < 0.55$ , while it is direct in the region  $r > 0.55$ , where in the first region the stress is positive, and it is negative otherwise. The stress increases as the radius of the inner tube increases which leads to reduce the area of fluid flow through the tube and thus it causes an increase in the pressure on the outer rubber tube wall. This behavior is observed in Figure 5d. We did not observe any effect of the parameter  $\lambda_1$  on the stress.

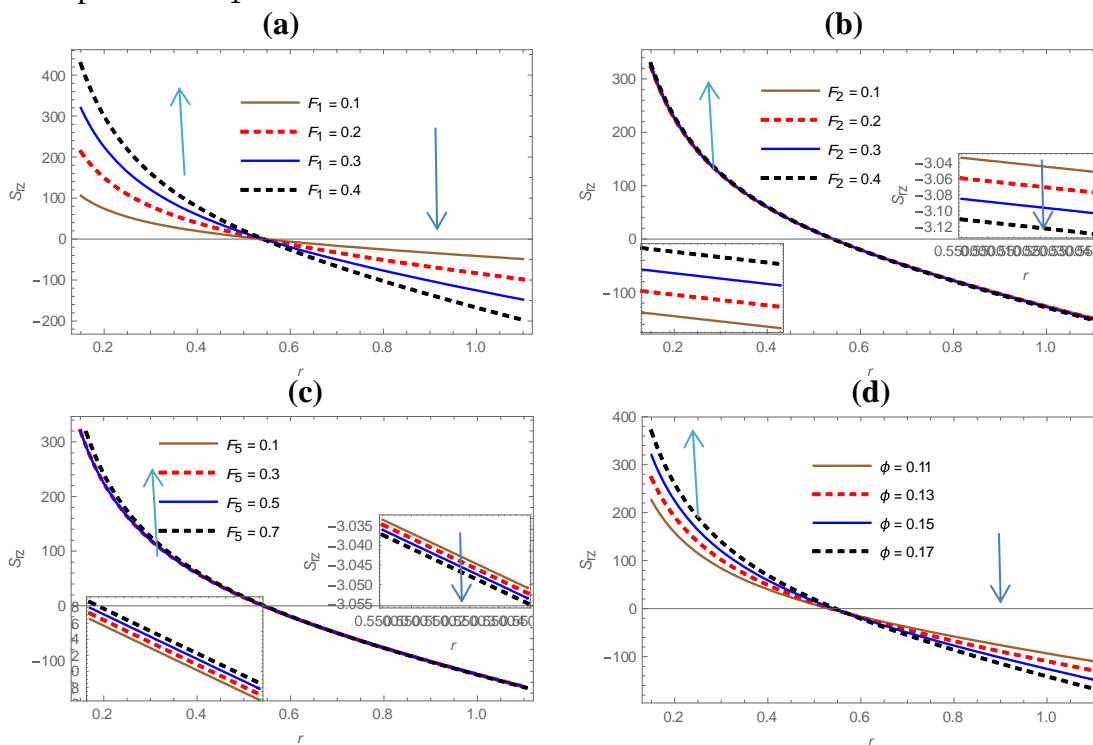


**Figure 4:** Stress distribution for various values of(a)  $F_1$ ,(b)  $F_2$  ,(c)  $\phi$  ,(d)  $F_5$  With  $\epsilon = 0.15, F_3 = 0.1, z = 0.5, F_4 = 0.5, \lambda_1 = 0.1, t = 0.1$

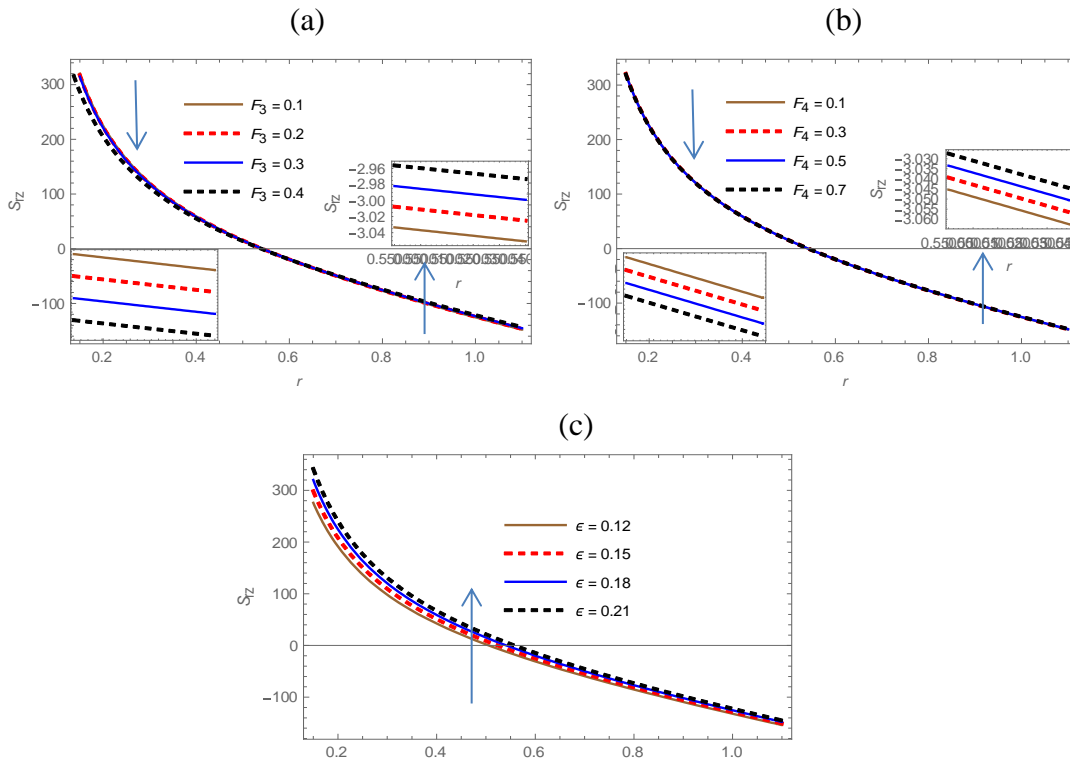


**Figure 5:** Stress distribution for various values of(a)  $F_3$ , (b)  $F_4$ , (c)  $\epsilon$  with  $\phi = 0.15$ ,  $F_1 = 0.3, z = 0.5, F_2 = 0.1, \lambda_1 = 0.1, t = 0.1$

**7.3 Phenomena Trapping**

A formation by closed streamlines of an internally circulating bolus of fluid is called trapping and the trapped bolus is pushed forward along with the peristaltic wave. Figures 6-13 illustrate the parameters of the results  $F_1, F_2, F_5, F_3, F_4, \lambda_1, \epsilon$ , and  $\phi$  on the trapped bolus. In Figures 6-8, We show the effect of parameters  $F_1, F_2$  and  $F_5$  on the trapped bolus. The volume of the trapped bolus located in the middle of the canal expands with an increase in  $F_1, F_2$  and  $F_5$ , respectively, where the bolus will turn into a wave. While in Figures 9-10, the size of the trapped bolus decreases with increasing parameters  $F_3$  and  $F_4$  in the middle of the channel gradually. The last Figures 11-13 in this research refer to the effect of the three parameters  $\lambda_1, \epsilon$ , and  $\phi$  on the trapped bolus, where we notice in Figure 11 that the bolus expands in size with an increase in  $\lambda_1$ , while in Fig 12 the bolus shrinks in size with an increase in  $\epsilon$ , and in the last Figure 13, we notice that the bolus expands and transforms from the center of the channel to its top at an acute angle and its shape turns from circular to oval with an increase in  $\phi$ .

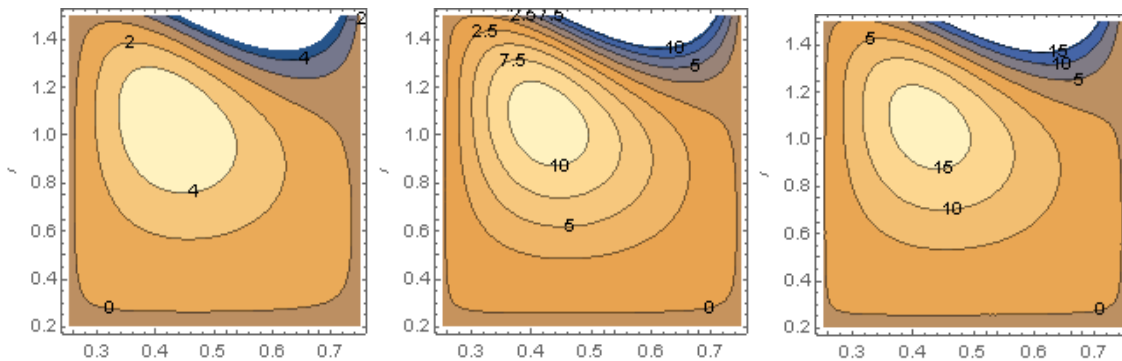


**Figure 6:** Wave frame streamlines for different values of  $F_1 = \{0.1, 0.2, 0.3\}$ ,  $\lambda_1 = 0.1, \epsilon = 0.15, \phi = 0.15, F_2 = 0.5, F_3 = 0.1, F_4 = 0.1, F_5 = 0.1, t = 0$



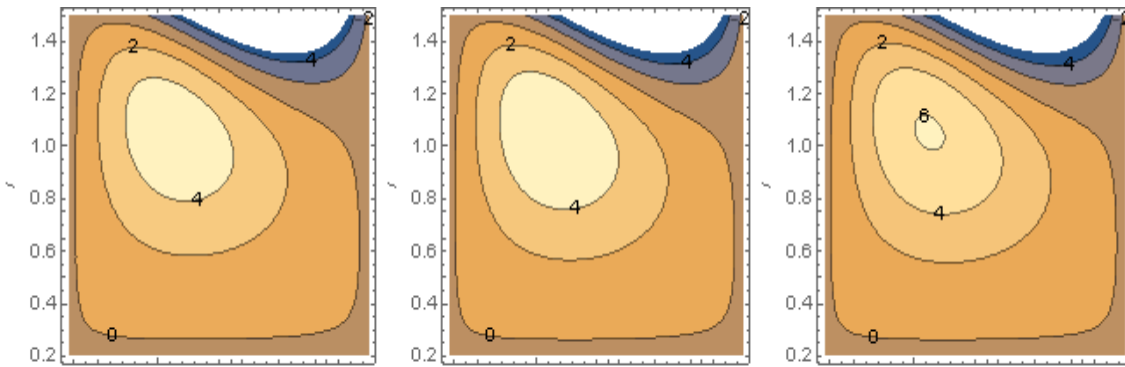


**Figure 7 :** Wave frame streamlines for different values of  $F_2=\{0.2,0.5,0.7\}$   
 $\lambda_1 = 0.1, \epsilon = 0.15, \phi = 0.15, F_1 = 0.1, F_3 = 0.1, F_4 = 0.1, F_5 = 0.1, t = 0$

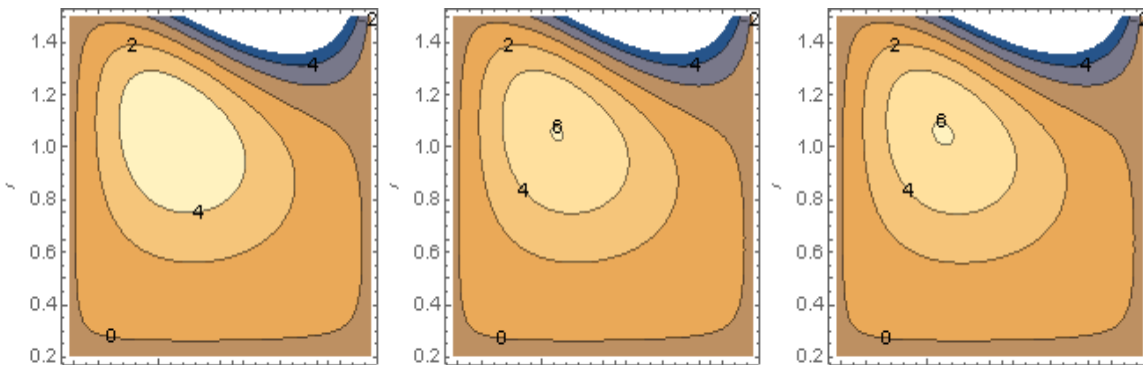


**Figure -8** Wave frame streamlines for different values of  $F_5=\{4,5,6\}$   
 $\lambda_1 = 0.1, \epsilon = 0.15, \phi = 0.15, F_1 = 0.1, F_2 = 0.5, F_3 = 0.1, F_4 = 0.1, t = 0$

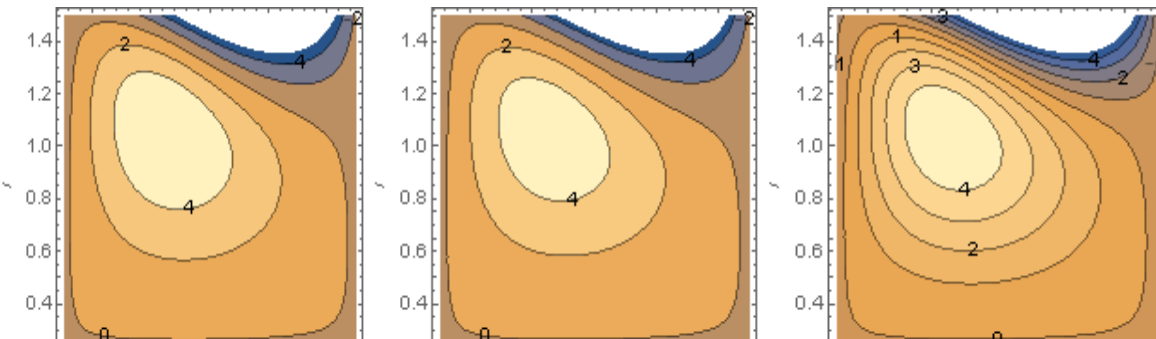


**Figure -9** Wave frame streamlines for different values of  $F_3=\{0.1,0.4,0.7\}$   
 $\lambda_1 = 0.1, \epsilon = 0.15, \phi = 0.15, F_1 = 0.1, F_2 = 0.5, F_4 = 0.1, F_5 = 0.1, t = 0$

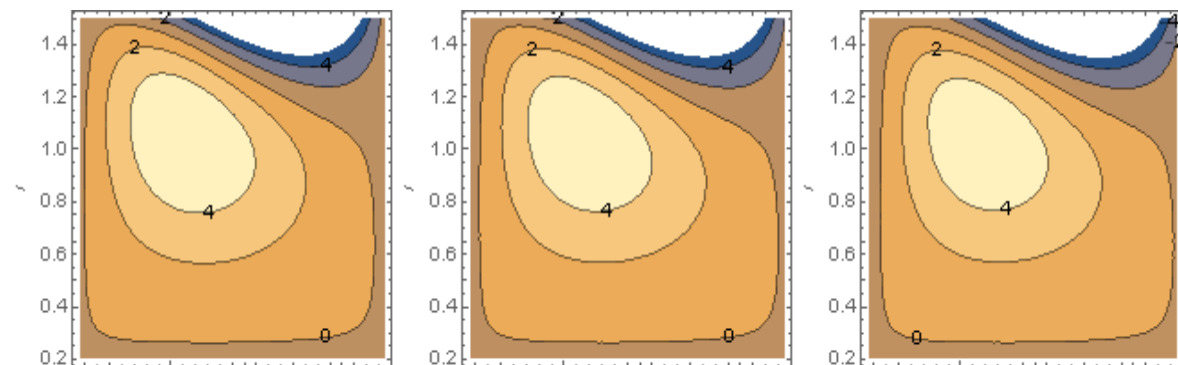


**Figure 10 :** Wave frame streamlines for different values of  $F_4=\{0.1,1.3,2.1\}$   
 $\lambda_1 = 0.1, \epsilon = 0.15, \phi = 0.15, F_1 = 0.1, F_2 = 0.5, F_3 = 0.1, F_5 = 0.1, t = 0$

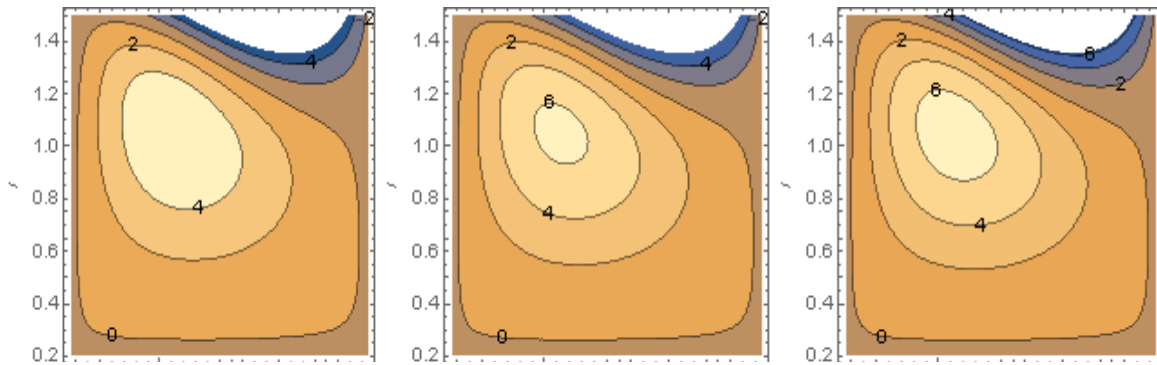


**Figure 11:** Wave frame streamlines for different values of  $\lambda_1 = \{0.1, 0.2, 0.3\}$   
 $\epsilon = 0.15, \phi = 0.15, F_1 = 0.1, F_2 = 0.5, F_3 = 0.1, F_4 = 0.1, F_5 = 0.1, t = 0$

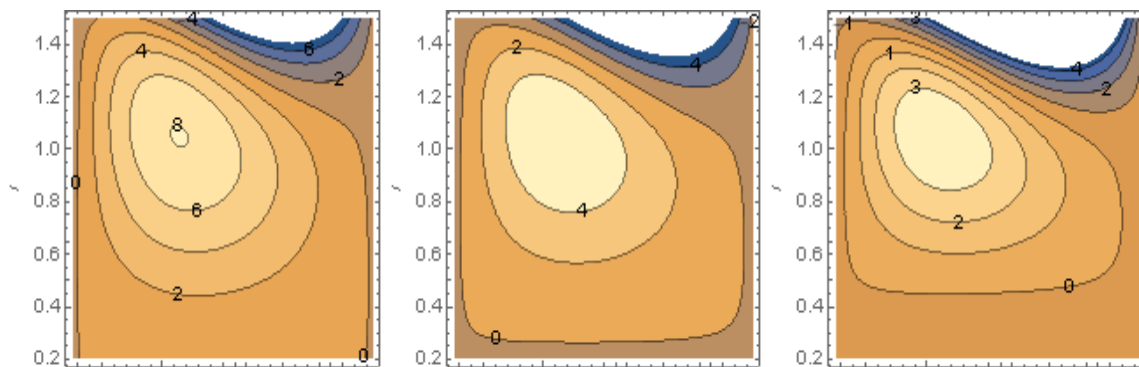


**Figure 12:** Wave frame streamlines for different values of  $\epsilon = \{0.05, 0.15, 0.25\}$   
 $\lambda_1 = 0.1, \phi = 0.15, F_1 = 0.1, F_2 = 0.5, F_3 = 0.1, F_4 = 0.1, F_5 = 0.1, t = 0$

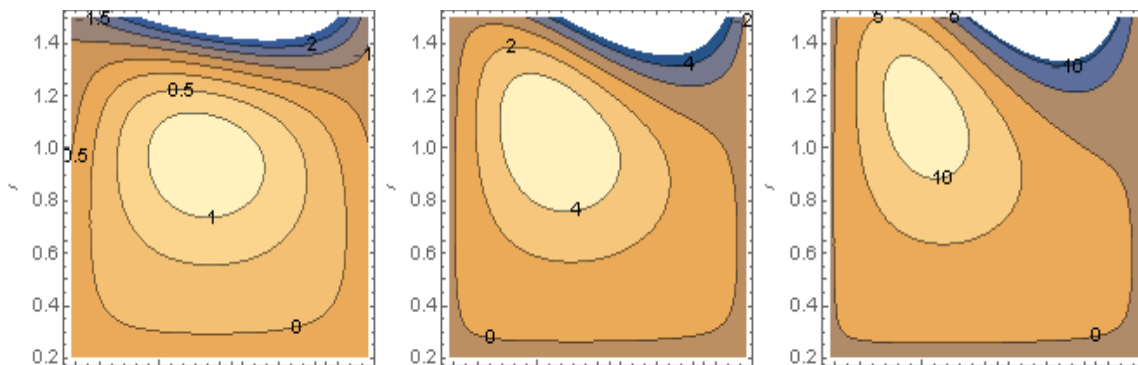


**Figure -13** Wave frame streamlines for different values of  $\phi = \{0.05, 0.15, 0.25\}$   
 $\lambda_1 = 0.1, \epsilon = 0.15, F_1 = 0.1, F_2 = 0.5, F_3 = 0.1, F_4 = 0.1, F_5 = 0.1, t = 0$

### 8. Concluding Remarks

We have obtained some important results by studying the effect of the peristaltic flow of Jeffrey’s fluid through a channel of two overlapping tubes having the same center, the inner is cylindrical is solid and the outer is elastic rubber, we will review briefly some of these results.

- The effect of parameters  $F_1, F_2, F_5, \lambda_1$ , and  $\phi$  on fluid velocity is direct, while the effect of parameters  $F_3, F_4$ , and  $\epsilon$  are indirect. In addition, we note that the parameters  $F_1, F_2, \lambda_1, \phi$ , and  $\epsilon$  have a high effect on fluid velocity, while the effect of  $F_4$  and  $F_5$  is weak.
- The stress is direct with the parameters  $F_1, F_2, F_5$  and  $\phi$  in the region  $r < 0.55$ , while inverse in the region  $r > 0.55$ , where in the first region the stress is positive while it is negative otherwise.

- The stress goes down with the parameters  $F_3$  and  $F_4$  in the region  $r < 0.55$  while rises in the region  $r > 0.55$ .
- The trapped bolus expands in size with an increase in  $F_1$ ,  $F_2$ ,  $F_5$ , and  $\lambda_1$ , while the bolus shrinks in size with an increase in  $F_3$ ,  $F_4$ , and  $\varepsilon$ .
- The trapped bolus expands and transforms from the center of the channel to its top at an acute angle and its shape turns from circular to oval, with an increase in  $\phi$ .

## References

- [1] Latham TW, "Liquid motions in a Peristaltic pump," *Massachusetts Institute of Technology*, 1966.
- [2] A. H. Shapiro, M. Y. Jaffrin and S. L. Weinberg, "Peristaltic pumping with long wavelengths at low Reynolds number" *Journal of Fluid Mechanics*, vol. 37, no. 4, pp. 799–825, 1969, doi: 10.1017/S0022112069000899.
- [3] T. S. Chow, "Peristaltic transport in a circular cylindrical pipe," *Journal of Applied Mechanics*, vol. 37, no. 4, pp. 901–905, 1970, doi: 10.1115/1.3408716.
- [4] S. Nadeem, A. Riaz and R. Ellahi, "Peristaltičko strujanje jeffrey-ovog fluida u pravougaonom kanalu sa popustljivim zidovima," *Chemical Industry and Chemical Engineering Quarterly*, vol. 19, no. 3, pp. 399–409, 2013, doi: 10.2298/CICEQ120402075N.
- [5] Dheia G. Salih Al-Khafajy, "Magnetohydrodynamic Peristaltic flow of a couple stress with heat and mass transfer of a Jeffery fluid in a tube through porous medium," *Advances in Physics Theories and Applications*, no. September, 2014.
- [6] A. A. Hussien Al-Aridhee and Dheia G. Salih Al-Khafajy, "Influence of MHD Peristaltic Transport for Jeffrey Fluid with Varying Temperature and Concentration through Porous Medium," *Journal of Advances in Physics.*, vol. 1294, no. 3, 2019, doi: 10.1088/1742-6596/1294/3/032012.
- [7] M. R. Salman and H. A. Ali, "Approximate treatment for the MHD peristaltic transport of jeffrey fluid in inclined tapered asymmetric channel with effects of heat transfer and porous medium," *Iraqi Journal of Science*, vol. 61, no. 12, pp. 3342–3354, 2020, doi: 10.24996/ijs.2020.61.12.22.
- [8] B. A. Almusawi and A. M. Abdulhadi, "Heat transfer analysis and magnetohydrodynamics effect on peristaltic transport of ree-eyring fluid in rotating frame," *Iraqi Journal of Science*, vol. 62, no. 8, pp. 2714–2725, 2021, doi: 10.24996/ijs.2021.62.8.25.
- [9] Dheia G. Salih Al-Khafajy and A. M. Abdulhadi, "Effects of MHD and wall properties on the peristaltic transport of a Carreau fluid through porous medium," *Journal of Advances in Physics*, vol. 6, no. 2, pp. 1106–1121, 2014, doi: 10.24297/jap.v6i2.1789.
- [10] G. C. Sankad and P. S. Nagathan, "Influence of Wall Properties on the Peristaltic Flow of a Jeffrey Fluid in a Uniform Porous Channel under Heat Transfer," *International Journal of Research in Industrial Engineering*, vol. 6, no. 6, pp. 246–261, 2017.
- [11] I. M. Eldesoky, R. M. Abumandour, M. H. Kamel and E. T. Abdelwahab, "The combined influences of heat transfer, compliant wall properties and slip conditions on the peristaltic flow through tube," *SN Applied Sciences*, vol. 1, no. 8, pp. 1–16, 2019, doi: 10.1007/s42452-019-0915-4.
- [12] S. Razzaq Al-Waily and Dheia G. Salih Al-Khafajy, "Magnetohydrodynamics Peristaltic Flow of a Couple- Stress with Varying Temperature and concentration for Jeffrey Fluid through a Flexible Porous Medium," *Al-Qadisiyah Journal Of Pure Science*, vol. 26, no. 4, pp. 466–484, 2021, doi: 10.29350/qjps.2021.26.4.1373.